

NASA TECHNICAL NOTE



NASA TN D-2450
C-1

NASA TN D-2450

LOAN COPY: RET
AFWL (WLIL)
KIRTLAND AFB, I



ON THE STABILITY OF A LIQUID LAYER
OF UNIFORM THICKNESS SPREAD OVER
A RIGID CIRCULAR CYLINDER SUBJECTED
TO LATERAL ACCELERATIONS

by Richard M. Beam
Ames Research Center
Moffett Field, Calif.



ON THE STABILITY OF A LIQUID LAYER OF UNIFORM THICKNESS
SPREAD OVER A RIGID CIRCULAR CYLINDER SUBJECTED
TO LATERAL ACCELERATIONS

By Richard M. Beam

Ames Research Center
Moffett Field, Calif.

NATIONAL AERONAUTICS AND SPACE ADMINISTRATION

For sale by the Office of Technical Services, Department of Commerce,
Washington, D.C. 20230 -- Price \$0.75

ON THE STABILITY OF A LIQUID LAYER OF UNIFORM THICKNESS

SPREAD OVER A RIGID CIRCULAR CYLINDER SUBJECTED

TO LATERAL ACCELERATIONS

By Richard M. Beam

Ames Research Center
Moffett Field, Calif.

SUMMARY

The equations of motion for a liquid layer of uniform thickness spread over a rigid circular cylinder subjected to lateral acceleration are derived. The liquid is assumed to be inviscid and incompressible and the analysis is restricted to the linearized (small deflection) equations of motion. The effect of surface tension of the liquid is included.

A modal solution of the equations of motion is obtained and the stability criterion for the liquid layer is derived. In addition, the criterion for maximum instability, or droplet formation, is derived. Both of these criteria are presented graphically as a plot of axial (along the axis of the cylinder) wave length versus Bond number. Correlation between a previous approximate theory and the present theory is presented. The available experimental data are compared with the theories.

INTRODUCTION

The transportation, storage, and utilization of liquids under near zero gravity conditions present many unanswered questions related to the operation of spacecraft and space stations. As the effective gravity field is diminished, the static and dynamic behavior of a liquid free surface is drastically changed since the interface surface tension forces become predominant.

Most investigators¹ to date have considered only the hydrostatic or equilibrium configurations of the free surface, while few have endeavored to increase the quite limited knowledge of the stability and dynamic characteristics of the free surface. The purpose of this report is to investigate in some detail a geometrically simple three-dimensional hydrodynamic problem and, thereby, to obtain qualitative and quantitative information which may lead to a basic understanding of this and more complicated problems.

The physical problem may be likened to the droplets formed on the underside of a telephone wire during a rain storm. The droplets appear to occur in a regular distribution along the length of the wire. The same phenomenon appears when the coolant tubes of a condenser are located in a horizontal position. One might wonder what (if any) change would occur in the droplet

¹Extensive bibliographies are contained in references 1 and 2.

distribution if the condenser were in a reduced gravity field and, in fact, if possibly under these conditions no droplets would form. Such a consideration has significance in connection with condensers carried on space vehicles.

This analytical work is an extension to three space dimensions of that reported by Anliker and Beam (ref. 1) which presented the two-dimensional analysis of the stability of a uniform liquid layer covering a rigid circular cylinder. An approximate solution to the three-dimensional problem was obtained by Lee (ref. 3) and a comparison will be made between his solution and the one contained herein.

In the following analysis, the liquid is assumed to be incompressible and inviscid and the flow is assumed to be irrotational. The density of the medium external to the liquid free surface is assumed to be negligible. The analysis is further restricted to the linearized (small deflection) equations of motion, a rigorous derivation of which is given in reference 1. The accuracy of the assumption of an inviscid fluid in the investigation of the small displacement stability seems to be validated in part by the work of Bellman and Pennington (ref. 4). They have shown that for flat layers, viscosity does not change the stability criterion but merely decreases the rate of growth for unstable wavelengths and causes damping for the stable (oscillatory) wavelengths. The essential discrepancy between the physical problems mentioned above and the mathematical problem is that the physical layer will not remain precisely at uniform thickness unless the appropriate external nonuniform (variation around circumference of layer) pressure distribution is applied. The applicability of this theoretical solution to the physical problems is then determined by the deviation of the equilibrium configuration from a uniformly thick layer. The available experimental data indicate, however, that the theory is applicable over a wide range of Bond number.

SYMBOLS

A_{mk}	constant defined by equation (28)
a	radius of equilibrium free surface
a_0	radius of rigid cylinder
B	Bond number, $\frac{\rho a^2 g}{\Gamma}$
b_m, \bar{b}_m	coefficients of Fourier series for antisymmetrical modes
c_m, \bar{c}_m	coefficients of Fourier series for symmetrical modes
g	effective gravity (lateral acceleration of rigid cylinder)
H_m	constant defined by equation (23)

I_m	modified Bessel function of the first kind of order m
j, k	integers
K_m	modified Bessel function of the second kind of order m
L_{cr}	wavelength corresponding to neutral stability of liquid layer
m, n	integers
P	matrix (eq. (42))
\bar{p}	pressure in liquid layer
$p_e(\theta)$	equilibrium pressure distribution applied at free surface
P_{ij}	constant defined by equation (44)
Q	matrix (eq. (42))
q_{ij}	constant defined by equation (43)
R	function introduced for separation of variables
R_1, R_2	radius of curvature of free surface
r	cylindrical coordinate (fig. 1)
S	bounding surface
T	surface tension coefficient
t	time variable
X	function introduced for separation of variables
x	cylindrical coordinate (fig. 1)
β	dimensionless wave number
β_{cr}	value of β corresponding to neutral stability of liquid layer
β_{max}	value of β corresponding to maximum instability of liquid layer
ϵ	ratio of cylinder radius to free surface radius, $\frac{a_0}{a}$
ζ	displacement of free surface from equilibrium configuration
Θ	function introduced for separation of variables

θ	cylindrical coordinate (fig. 1)
λ_1	axial wave number
λ_2	separation constant
ρ	liquid density
$\sigma, \bar{\sigma}$	frequency parameter (eq. (31))
Φ	potential function
Ψ	potential function in terms of space variables
Ω	potential of body forces

ANALYSIS

The mathematical model is formulated by considering the motion of a liquid layer of uniform thickness spread over a rigid nonporous circular cylinder (fig. 1). The cylindrical coordinates will be denoted by x , the distance along the axis of the cylinder; θ , the angular displacement measured from the vertical; and r , the radial distance from the axis of the cylinder. The radius of the rigid cylinder is a_0 and the radius of the equilibrium free surface of the liquid layer is a . The radial displacement of the free surface from its equilibrium position is denoted by ζ . The body forces acting on the fluid (due to lateral acceleration of the cylinder) are normal to the axis of the cylinder and parallel to the plane $\theta = 0$ as indicated in figure 1. It is assumed that the liquid wets the rigid cylinder.

The potential equation for incompressible irrotational flow is, in cylindrical coordinates,

$$\nabla^2 \Phi(r, x, \theta, t) = \Phi_{rr} + \frac{1}{r} \Phi_r + \frac{1}{r^2} \Phi_{\theta\theta} + \Phi_{xx} = 0 \quad (1)$$

where Φ is the velocity potential of the fluid, t the time variable, and a subscript represents partial differentiation with respect to that variable. The dynamic boundary condition at the free surface ($r = a + \zeta$) is

$$\bar{p} \Big|_{r=a+\zeta} - p_e = T \left(\frac{1}{R_1} + \frac{1}{R_2} \right) \quad (2)$$

where \bar{p} is the pressure in the liquid layer, p_e the external applied equilibrium pressure, T the surface tension (force per unit length) and R_1, R_2 the principal radii of curvature of the free surface. The kinematic boundary condition of a surface may be written

$$\frac{DS}{Dt} = 0 \quad (3)$$

with $S = 0$ the equation of the bounding surface. At the rigid cylinder surface ($S_c = r - a_0 = 0$) there is no flow through the boundary

$$\left. \frac{DS_c}{Dt} = -\Phi_r \right|_{r=a_0} = 0 \quad (4)$$

and at the interface surface ($S_i = r - a - \zeta = 0$) there is no flow across the surface

$$\frac{DS_i}{Dt} = -\Phi_r - \frac{\partial \zeta}{\partial t} + \frac{\partial \zeta}{\partial \theta} \frac{\Phi_\theta}{r^2} + \frac{\partial \zeta}{\partial x} \Phi_x = 0$$

which after elimination of nonlinear terms becomes

$$\left. \Phi_r \right|_{r=a} = - \frac{\partial \zeta}{\partial t} \quad (5)$$

The pressure, \bar{p} , is given by the linearized Bernoulli equation (ref. 1)

$$\bar{p} = \rho \left(\frac{\partial \Phi}{\partial t} - \Omega \right) \quad (6)$$

where ρ denotes the liquid density, and Ω , the potential of the body forces, is given by

$$\Omega = gr \cos \theta \quad (7)$$

with g representing the effective gravity field coefficient (or the acceleration of the rigid cylinder).

The linearized expressions for the principal radii of curvature R_1 and R_2 are (see ref. 1)

$$\frac{1}{R_1} = - \frac{\partial^2 \zeta}{\partial x^2} \quad (8)$$

$$\frac{1}{R_2} = \frac{1}{a} \left(1 - \frac{\zeta}{a} - \frac{1}{a} \frac{\partial^2 \zeta}{\partial \theta^2} \right) \quad (9)$$

The appropriate substitutions from equations (6), (7), (8), and (9) into equation (2) lead to

$$\rho \left[\frac{\partial \Phi}{\partial t} - g(a + \zeta) \cos \theta \right] - p_e = T \left[- \frac{\partial^2 \zeta}{\partial x^2} + \frac{1}{a} \left(1 - \frac{\zeta}{a} - \frac{1}{a} \frac{\partial^2 \zeta}{\partial \theta^2} \right) \right] \quad (10)$$

which is a combination of the kinematic and dynamic boundary conditions which must be satisfied at the free surface ($r = a + \zeta$) or, to the first approximation, at the equilibrium free surface ($r = a$). From relation (10) one may obtain the pressure distribution which must be applied to the equilibrium free surface to maintain a uniform liquid layer; namely

$$p_e = -\frac{T}{a} - \rho g a \cos \theta \quad (11)$$

Differentiating both sides of equation (10) with respect to time and substituting $\partial \zeta / \partial t$ from expression (5) result in

$$\rho \left(\frac{\partial^2 \Phi}{\partial t^2} + g \Phi_r \cos \theta \right)_{r=a} = T \left[\Phi_{rxx} + \frac{1}{a^2} (\Phi_r + \Phi_{\theta\theta r}) \right]_{r=a} \quad (12)$$

The velocity potential Φ must satisfy differential equation (1) and the boundary conditions (4) and (12). With the separation of the time and space variables by the substitution

$$\Phi(r, x, \theta, t) = e^{i\sqrt{\sigma}t} \Psi(r, x, \theta) \quad (13)$$

into equations (1), (4), and (12), the stability problem is reduced to the eigenvalue problem

$$\Psi_{rr} + \frac{1}{r} \Psi_r + \frac{1}{r^2} \Psi_{\theta\theta} + \Psi_{xx} = 0 \quad (14)$$

$$\rho \left(-\sigma \Psi + g \Psi_r \cos \theta \right)_{r=a} = T \left[\Psi_{xxr} + \frac{1}{a^2} (\Psi_r + \Psi_{\theta\theta r}) \right]_{r=a} \quad (15)$$

$$\left(\Psi_r \right)_{r=a_0} = 0 \quad (16)$$

where σ is the eigenvalue and Ψ the eigenfunction. If σ is complex, or real and negative, then Φ increases without limit as time increases and is therefore unstable. If σ is real and positive, then Φ is oscillatory with time and the amplitude depends on the initial conditions or external disturbances; thus the motion is stable. The stability criterion requires that σ be real and positive.

Separation of the space variables by the substitution

$$\Psi = R(r) X(x) \Theta(\theta) \quad (17)$$

into equation (14) leads to the following ordinary differential equations

$$X'' + \lambda_1 X = 0 \quad (18)$$

$$\Theta'' + \lambda_2 \Theta = 0 \quad (19)$$

$$R'' + \frac{1}{r} R' - \left(\lambda_1 + \frac{\lambda_2}{r^2} \right) R = 0 \quad (20)$$

where λ_1 and λ_2 are separation constants. (The two-dimensional problem considered in reference 1 is obtained by setting $\lambda_1 = 0$.) The function Ψ obtained in this manner will not, however, satisfy the free surface boundary condition given by equation (15) because of the variable coefficient $\cos \theta$. The following procedure will be used to construct Ψ as a Fourier series in θ . Each term of the series will satisfy equation (14) and the boundary condition at the rigid cylinder wall, equation (16). The coefficients of the Fourier series will be chosen so that the interface boundary condition (15) will be satisfied. In this manner Ψ is chosen of the form

$$\Psi = \sum_{m=0}^{\infty} \left[I_m(\lambda_1 r) - \frac{I_m'(\lambda_1 a_0)}{K_m'(\lambda_1 a_0)} K_m(\lambda_1 r) \right] e^{i\lambda_1 x} (c_m \cos m\theta + b_m \sin m\theta) \quad (21)$$

where I_m and K_m represent the m th order modified Bessel functions of the first and second kind, respectively, and c_m and b_m are constants to be determined. The separation variable λ_2 in equation (19) was replaced by the integer m to insure physical continuity at $\theta = 0, 2\pi$. A prime has been used to denote differentiation with respect to the argument of the function. The substitution of Ψ from equation (21) into the free surface boundary condition (15) results in

$$\begin{aligned} & \rho \left\{ -\sigma \sum_{m=0}^{\infty} \left[I_m(\lambda_1 a) - \frac{I_m'(\lambda_1 a_0)}{K_m'(\lambda_1 a_0)} K_m(\lambda_1 a) \right] \left[c_m \cos(m\theta) + b_m \sin(m\theta) \right] e^{i\lambda_1 x} \right. \\ & + g \cos \theta \sum_{m=0}^{\infty} \lambda_1 \left[I_m'(\lambda_1 a) - \frac{I_m'(\lambda_1 a_0)}{K_m'(\lambda_1 a_0)} K_m'(\lambda_1 a) \right] \left[c_m \cos(m\theta) + b_m \sin(m\theta) \right] e^{i\lambda_1 x} \left. \right\} \\ & = T \left\{ \sum_{m=0}^{\infty} -\lambda_1^3 \left[I_m'(\lambda_1 a) - \frac{I_m'(\lambda_1 a_0)}{K_m'(\lambda_1 a_0)} K_m'(\lambda_1 a) \right] \left[c_m \cos(m\theta) + b_m \sin(m\theta) \right] e^{i\lambda_1 x} \right. \\ & + \frac{1}{a^2} \sum_{m=0}^{\infty} \lambda_1 \left[I_m'(\lambda_1 a) - \frac{I_m'(\lambda_1 a_0)}{K_m'(\lambda_1 a_0)} K_m'(\lambda_1 a) \right] \left[c_m \cos(m\theta) + b_m \sin(m\theta) \right] e^{i\lambda_1 x} \\ & + \frac{1}{a^2} \sum_{m=0}^{\infty} -\lambda_1 m^2 \left[I_m'(\lambda_1 a) - \frac{I_m'(\lambda_1 a_0)}{K_m'(\lambda_1 a_0)} K_m'(\lambda_1 a) \right] \left[c_m \cos(m\theta) + b_m \sin(m\theta) \right] e^{i\lambda_1 x} \left. \right\} \end{aligned} \quad (22)$$

With the definitions

$$H_m = \frac{I_m(\lambda_1 a) K_m'(\lambda_1 a_0) - I_m'(\lambda_1 a_0) K_m(\lambda_1 a)}{I_m'(\lambda_1 a) K_m'(\lambda_1 a_0) - I_m'(\lambda_1 a_0) K_m'(\lambda_1 a)} \quad (23)$$

$$\bar{c}_m = \left[I_m'(\lambda_1 a) - \frac{I_m'(\lambda_1 a_0)}{K_m'(\lambda_1 a_0)} K_m'(\lambda_1 a) \right] c_m \quad (24)$$

$$\bar{b}_m = \frac{\bar{c}_m}{c_m} b_m \quad (25)$$

equation (22) may be simplified to

$$\begin{aligned} \rho \left\{ - \sigma \sum_{m=0}^{\infty} H_m e^{i\lambda_1 x} \left[\bar{c}_m \cos(m\theta) + \bar{b}_m \sin(m\theta) \right] \right. \\ \left. + g \cos \theta \sum_{m=0}^{\infty} \lambda_1 e^{i\lambda_1 x} \left[\bar{c}_m \cos(m\theta) + \bar{b}_m \sin(m\theta) \right] \right\} \\ = T \left\{ \sum_{m=0}^{\infty} - \lambda_1^3 e^{i\lambda_1 x} \left[\bar{c}_m \cos(m\theta) + \bar{b}_m \sin(m\theta) \right] \right. \\ \left. + \frac{1}{a^2} \sum_{m=0}^{\infty} \lambda_1 e^{i\lambda_1 x} \left[\bar{c}_m \cos(m\theta) + \bar{b}_m \sin(m\theta) \right] \right. \\ \left. + \frac{1}{a^2} \sum_{m=0}^{\infty} - \lambda_1 m^2 e^{i\lambda_1 x} \left[\bar{c}_m \cos(m\theta) + \bar{b}_m \sin(\theta) \right] \right\} \quad (26) \end{aligned}$$

The equations for \bar{c}_m are obtained by multiplying equation (26) by $\cos(k\theta)d\theta$ ($k = 0, 1, \dots$) and integrating from 0 to π which produces

$$\rho \left[- \sigma H_k e^{i\lambda_1 x} \frac{\pi}{2} \bar{c}_k + g \sum_{m=0}^{\infty} \lambda_1 e^{i\lambda_1 x} A_{mk} \bar{c}_m \right] = T \left\{ \left[- \lambda_1^3 + \frac{\lambda_1}{a^2} (1 - k^2) \right] \frac{\pi}{2} e^{i\lambda_1 x} \bar{c}_k \right\} \quad (27)$$

where

$$\left. \begin{aligned} A_{mk} &= \int_0^{\pi} \cos \theta \cos(m\theta) \cos(k\theta) d\theta = 0 & m \neq k \pm 1 \\ &= \frac{\pi}{4} & m = k \pm 1 \end{aligned} \right\} \quad (28)$$

Since equation (27) is to be valid for all values of x , the common factor $e^{i\lambda_1 x}$ may be omitted

$$\left\{ -\sigma H_k - \frac{T}{\rho} \left[-\lambda_1^3 + \frac{\lambda_1}{a^2} (1 - k^2) \right] \right\} \bar{c}_k + \frac{2}{\pi} g \lambda_1 \sum_{m=0}^{\infty} A_{mk} \bar{c}_m = 0 \quad k = 0, 1, 2, \dots \quad (29)$$

In a similar manner the equations for \bar{b}_m are obtained by multiplying equation (26) by $\sin(k\theta)d\theta$ and integrating from 0 to π ; thus,

$$\left\{ -\sigma H_k - \frac{T}{\rho} \left[-\lambda_1^3 + \frac{\lambda_1}{a^2} (1 - k^2) \right] \right\} \bar{b}_k + \frac{2}{\pi} g \lambda_1 \sum_{m=1}^{\infty} A_{mk} \bar{b}_m = 0 \quad k = 1, 2, \dots \quad (30)$$

which are identical to those for \bar{c}_m except for the range of summation index. The \bar{c}_m corresponds to symmetrical modes (symmetrical about $\theta = 0$) and the \bar{b}_m corresponds to the antisymmetrical modes.

It is convenient to make equations (23), (29), and (30) dimensionless by the following substitutions

$$\bar{\sigma} = \frac{\rho a^3}{T} \sigma \quad (31)$$

$$\beta = \lambda_1 a \quad (32)$$

$$\epsilon = \frac{a_0}{a} \quad (33)$$

$$B = \frac{\rho a^2 g}{T} \quad (34)$$

and the final equations for \bar{c}_m and \bar{b}_m are

$$\left\{ \bar{\sigma} \frac{1}{\beta} H_k(\beta) - \left[\beta^2 + (k^2 - 1) \right] \right\} \bar{c}_k - \frac{2}{\pi} B \sum_{m=0}^{\infty} A_{mk} \bar{c}_m = 0 \quad k = 0, 1, 2, \dots \quad (35)$$

and

$$\left\{ \bar{\sigma} \frac{1}{\beta} H_k(\beta) - \left[\beta^2 + (k^2 - 1) \right] \right\} \bar{b}_k - \frac{2}{\pi} B \sum_{m=1}^{\infty} A_{mk} \bar{b}_m = 0 \quad k = 1, 2, 3, \dots \quad (36)$$

For purposes of clarity equations (35) and (36) are displayed in the following matrix form

$$\begin{bmatrix}
 \bar{\sigma} \frac{H_0(\beta)}{\beta} - [\beta^2 + (0-1)] & -\frac{B}{2} & 0 & 0 & \cdot \\
 -\frac{B}{2} & \bar{\sigma} \frac{H_1(\beta)}{\beta} - [\beta^2 + (1-1)] & -\frac{B}{2} & 0 & \cdot \\
 0 & -\frac{B}{2} & \bar{\sigma} \frac{H_2(\beta)}{\beta} - [\beta^2 + (4-1)] & -\frac{B}{2} & \cdot \\
 0 & 0 & -\frac{B}{2} & \bar{\sigma} \frac{H_3(\beta)}{\beta} - [\beta^2 + (9-1)] & \cdot \\
 \cdot & \cdot & \cdot & \cdot & \cdot
 \end{bmatrix}
 \begin{Bmatrix}
 \bar{c}_0 \\
 \bar{c}_1 \\
 \bar{c}_2 \\
 \bar{c}_3 \\
 \cdot
 \end{Bmatrix}
 =
 \begin{Bmatrix}
 0 \\
 0 \\
 0 \\
 0 \\
 0
 \end{Bmatrix}
 \quad (37)$$

and

$$\begin{bmatrix}
 \bar{\sigma} \frac{H_1(\beta)}{\beta} - [\beta^2 + (1-1)] & -\frac{B}{2} & 0 & 0 & \cdot \\
 -\frac{B}{2} & \bar{\sigma} \frac{H_2(\beta)}{\beta} - [\beta^2 + (4-1)] & -\frac{B}{2} & 0 & \cdot \\
 0 & -\frac{B}{2} & \bar{\sigma} \frac{H_3(\beta)}{\beta} - [\beta^2 + (9-1)] & -\frac{B}{2} & \cdot \\
 0 & 0 & -\frac{B}{2} & \bar{\sigma} \frac{H_4(\beta)}{\beta} - [\beta^2 + (16-1)] & \cdot \\
 \cdot & \cdot & \cdot & \cdot & \cdot
 \end{bmatrix}
 \begin{Bmatrix}
 \bar{b}_1 \\
 \bar{b}_2 \\
 \bar{b}_3 \\
 \bar{b}_4 \\
 \cdot
 \end{Bmatrix}
 =
 \begin{Bmatrix}
 0 \\
 0 \\
 0 \\
 0 \\
 \cdot
 \end{Bmatrix}
 \quad (38)$$

There are two sets of linear, homogeneous, simultaneous equations for the coefficients \bar{c}_m and \bar{b}_m ; therefore a nontrivial solution exists only if the determinants of the coefficients of equations (37) and (38) are equal to zero. The eigenvalue problem for $\bar{\sigma}$ has been defined

$$\begin{vmatrix}
 \bar{\sigma} \frac{H_0(\beta)}{\beta} - [\beta^2 + (0-1)] & -\frac{B}{2} & 0 & 0 & \cdot \\
 -\frac{B}{2} & \bar{\sigma} \frac{H_1(\beta)}{\beta} - [\beta^2 + (1-1)] & -\frac{B}{2} & 0 & \cdot \\
 0 & -\frac{B}{2} & \bar{\sigma} \frac{H_2(\beta)}{\beta} - [\beta^2 + (4-1)] & -\frac{B}{2} & \cdot \\
 0 & 0 & -\frac{B}{2} & \bar{\sigma} \frac{H_3(\beta)}{\beta} - [\beta^2 + (9-1)] & \cdot \\
 \cdot & \cdot & \cdot & \cdot & \cdot
 \end{vmatrix}
 = 0
 \quad (39)$$

for the symmetrical modes, and

$$\begin{vmatrix}
 \bar{\sigma} \frac{H_1(\beta)}{\beta} - [\beta^2 + (1 - 1)] & -\frac{B}{2} & 0 & 0 & \cdot \\
 -\frac{B}{2} & \bar{\sigma} \frac{H_2(\beta)}{\beta} - [\beta^2 + (4 - 1)] & -\frac{B}{2} & 0 & \cdot \\
 0 & -\frac{B}{2} & \bar{\sigma} \frac{H_3(\beta)}{\beta} - [\beta^2 + (9 - 1)] & -\frac{B}{2} & \cdot \\
 0 & 0 & -\frac{B}{2} & \bar{\sigma} \frac{H_4(\beta)}{\beta} - [\beta^2 + (16 - 1)] & \cdot \\
 \cdot & \cdot & \cdot & \cdot & \cdot
 \end{vmatrix} = 0$$

(40)

for the antisymmetrical modes.

Stability Boundary

The stability boundary will be defined as the boundary between regions of the $\beta - B$ plane which correspond to stable and unstable motion of the liquid layer. The boundary will be denoted by β_{cr} and the critical wavelength by

$$L_{cr} = \frac{2\pi a}{\beta_{cr}} \quad (41)$$

L_{cr} is the minimum length of cylinder for which the liquid layer will be unstable. As will be shown in the next section, L_{cr} is not necessarily (and, in fact, not usually) the distance between droplets.

The stability boundary is found in the following manner. Denote the frequency determinants (39) and (40) by

$$|Q\bar{\sigma} - P| = 0 \quad (42)$$

where Q and P are matrices whose elements q_{ij} and p_{ij} are defined as

$$\left. \begin{aligned} q_{ij} &= + \frac{H_i}{\beta} & i = j \\ &= 0 & i \neq j \end{aligned} \right\} \quad (43)$$

$$\left. \begin{aligned} p_{ij} &= +[\beta^2 + (i^2 - 1)]\beta & i = j \\ &= + \frac{B}{2} & i = j \pm 1 \\ &= 0 & i \neq j \pm 1, i \neq j \end{aligned} \right\} \quad (44)$$

Since Q and P are symmetric matrices and Q is positive definite, then all values of $\bar{\sigma}$ are real (ref. 5). The stability criterion that $\bar{\sigma}$ be real and positive may be replaced by the simpler criterion that $\bar{\sigma}$ be positive. The stability boundary is the maximum value of β (minimum value of L) for which $\bar{\sigma} = 0$. This is accomplished by substituting $\bar{\sigma} = 0$ into equations (39) and (40)

$$\begin{vmatrix} \beta^2 + (0 - 1) & \frac{B}{2} & 0 & 0 & \cdot \\ \frac{B}{2} & \beta^2 + (1 - 1) & \frac{B}{2} & 0 & \cdot \\ 0 & \frac{B}{2} & \beta^2 + (4 - 1) & \frac{B}{2} & \cdot \\ 0 & 0 & \frac{B}{2} & \beta^2 + (9 - 1) & \cdot \\ \cdot & \cdot & \cdot & \cdot & \cdot \end{vmatrix} = 0 \quad (45)$$

$$\begin{vmatrix} \beta^2 + (1 - 1) & \frac{B}{2} & 0 & 0 & \cdot \\ \frac{B}{2} & \beta^2 + (4 - 1) & \frac{B}{2} & 0 & \cdot \\ 0 & \frac{B}{2} & \beta^2 + (9 - 1) & \frac{B}{2} & \cdot \\ 0 & 0 & \frac{B}{2} & \beta^2 + (16 - 1) & \cdot \\ \cdot & \cdot & \cdot & \cdot & \cdot \end{vmatrix} = 0 \quad (46)$$

and evaluating $\beta(B)$ by assuming values of B and finding the corresponding values of β from these new eigenvalue problems. An 8×8 (eight rows and eight columns) approximation² was used for the infinite determinants. The results of this numerical exercise, which was performed on a digital computer, are presented in figure 2. The even numbered β 's (β_0, β_2, \dots) correspond to the symmetric modes and the odd numbered (β_1, β_3, \dots) to the antisymmetric modes. The stability boundary β_{cr} is identical to β_0 since above this boundary ($\beta > \beta_0$), all values of $\bar{\sigma}$ are positive or, correspondingly, P is positive definite.

The symmetrical and antisymmetrical mode shapes (θ variation) corresponding to the lowest ordered β (β_0 and β_1 , respectively) are plotted in figure 4. These mode shapes were obtained by substituting the appropriate values for β , B , and σ ($\sigma = 0$) into equations (37) and (38) to obtain the c_n and b_n . The θ variation of the mode shapes was then obtained by the summations $\sum_{n=0}^7 \bar{c}_n \cos n\theta$ and $\sum_{n=1}^8 \bar{b}_n \sin n\theta$.

An appropriate experimental check on the stability boundary would be a systematic increase of cylinder length (keeping the interface radius constant) until droplets appeared. Another approach would, of course, be to keep the length fixed while increasing the interface radius. Experimental data of this type apparently have not been obtained.

Considering thin layers ($a_0/a \approx 1$) and assuming a symmetrical mode shape, Lee (ref. 3) obtained an approximate expression for the stability boundary; namely,

$$\beta_{cr} \approx \sqrt{B^2 - 1} \quad (47)$$

Lee's approximation and the present theory are compared in figure 5. For $B < 4$ the character of the two solutions is quite different. Lee's solution implies that if $B < 1$, the layer is stable. The present theory shows β_{cr} intersecting the β axis at $\beta = 1$ which is in agreement with Rayleigh's (ref. 6, p. 473) solution for a liquid jet (no effective gravity, $B = 0$, and no rigid cylinder, $a_0 = 0$) where the critical wavelength is $L_{cr} = 2\pi a$.

Droplet Formation

Although the stability boundary, β_{cr} , separates stable and unstable values of β , it does not necessarily determine the wavelength at which droplets will form. If the layer is unbounded in the x coordinate (i.e., the

²The convergence of the β 's, as the size ($n \times n$) of the approximating determinant is increased, is illustrated in a plot of β versus $1/n$ for the symmetrical modes (fig. 3). The 8×8 approximation is equivalent to retaining a sixteenth-order polynomial for β or an eighth-order polynomial for β^2 . The real roots of the polynomial are the desired β values and are, therefore, those values plotted in figure 3.

length of the cylinder is much greater than the radius of the interface surface), there is a value of β , to be denoted β_{\max} , for which $\bar{\sigma}$ has a maximum negative value (i.e., a maximum instability).³ Theoretically this is the value of β at which droplets will appear.⁴ The validity of this linear analysis in predicting the droplet formation must be ascertained by a nonlinear (large deflection) analysis or by experiment. The experimental work of Lee (ref. 3) has shown that linear theory is sufficient to predict droplet formation for $B > 4$; however, for $B < 4$ experimental data are, at present, insufficient for definite conclusions to be drawn.

The β_{\max} curve was evaluated numerically for two ratios of rigid cylinder radius to interface radius ($\epsilon = a_0/a$). The values, $\epsilon = 0.0, 0.9$, were chosen to be typical of the whole range $0 \leq \epsilon < 1$. The negative maximum value of $\bar{\sigma}$ was obtained by taking an 8×8 approximation for the frequency equations (39) and (40). The resulting β_{\max} , $(d\bar{\sigma}/d\beta) = 0$, curves are shown in figure 5. In this same figure Lee's approximate curve is shown for comparison. The analytical expression for Lee's solution is

$$\beta_{\max} \approx \frac{\sqrt{B^2 - 1}}{\sqrt{3}} \quad (48)$$

The experimental data presented by Lee are plotted in figure 5. For $B > 4$, theory and experiment agree well,⁵ however, for $B < 4$ the experimental data are not so complete as to warrant final comparison; therefore, more experimental data points are required in this region.

³For the purposes of clarity, a sketch of $\bar{\sigma}(\beta)$ for constant B is presented in figure 6. The β_{cr} as well as the β_{\max} value is indicated. The sketch corresponds to $\sqrt{B} \approx 3$.

⁴The argument is that if the response is proportional to a series of exponential terms (e^{bt}) and the system is given a general disturbance, then the term with the largest exponential factor b will eventually predominate.

⁵Lee's data was for thin layers. Although he did not specify the thickness, photographs of the experiments indicate that $\epsilon = 0.9$ is a reasonable assumption.

It should be noted that in his experiments, Lee used a wick at the top of the cylinder ($\theta = 0$) which provided a boundary condition not taken into account in the theory. Conclusive experimental data should be obtained without obstructions in contact with the cylinder. It should also be remembered that the criterion for droplet formation (from the analysis of Lee and the present analysis) is based on the assumption of an infinitely long cylinder. Thus when the distance between droplets is of the same order of magnitude as the length of the cylinder, the end effects may be important. It is interesting to note that for the two data points corresponding to $B \approx 1.2$ and 1.6 (fig. 5), the ratios of test cylinder length to distance between droplets are integer values (7 and 8, respectively). In order to meet the physical requirements at the ends of the tube, the number of wavelengths must, of course, be integer values.

CONCLUDING REMARKS

The stability criterion for a liquid layer of uniform thickness spread over a rigid circular cylinder subjected to lateral acceleration has been established according to the linear theory. The criterion for maximum instability, or droplet formation, of the unbounded (infinitely long) liquid layer has been determined. No experimental data are presently available for the stability boundary. Experimental data for droplet formation are available for Bond numbers $1 < B < 100$. For $B > 2$, theory and experiment agree well for droplet formation. Since the experimental data for $B < 2$ are quite limited and somewhat questionable (because of the ratio of the test cylinder length to distance between droplets), more experimental data on droplet formation are required if the comparison of theory and experiment is to be conclusive. The analysis contained in this report is readily adaptable to the study of a liquid layer spread over the inside of rigid circular cylinders, such as space vehicle propellant tanks exposed to low gravity environments. The stability criterion (fig. 2) is directly applicable but the maximum instability criterion (fig. 5) must be recalculated.

Ames Research Center
National Aeronautics and Space Administration
Moffett Field, Calif., June 2, 1964

REFERENCES

1. Anliker, Max, and Beam, R. M.: On the Stability of Liquid Layers Spread Over Simple Curved Bodies. Jour. Aerospace Sci., vol. 29, no. 10, Oct. 1962, pp. 1196-1209.
2. Reynolds, W. C.: Hydrodynamic Considerations for the Design of Systems for Very Low Gravity Environments. Tech. Rep. LG-1, Sept. 1, 1961, Stanford University Department of Mechanical Engineering.
3. Lee, Shao-Lin: Taylor Instability of a Liquid Film Around a Long, Horizontal, Circular Cylindrical Body in Still Air. Jour. Appl. Mech., vol. 30, Sept. 1963, pp. 443-7.
4. Pennington, R.: Machine Calculation of the Growth of Taylor Instability in an Incompressible Fluid. Princeton U., N.J., No. PNJ-LA-11, 1953.
5. Hildebrand, F. B.: Methods of Applied Mathematics. Prentice-Hall, N.Y., 1952.
6. Lamb, Sir Horace: Hydrodynamics. Sixth ed., Dover Publications, N.Y., 1945.

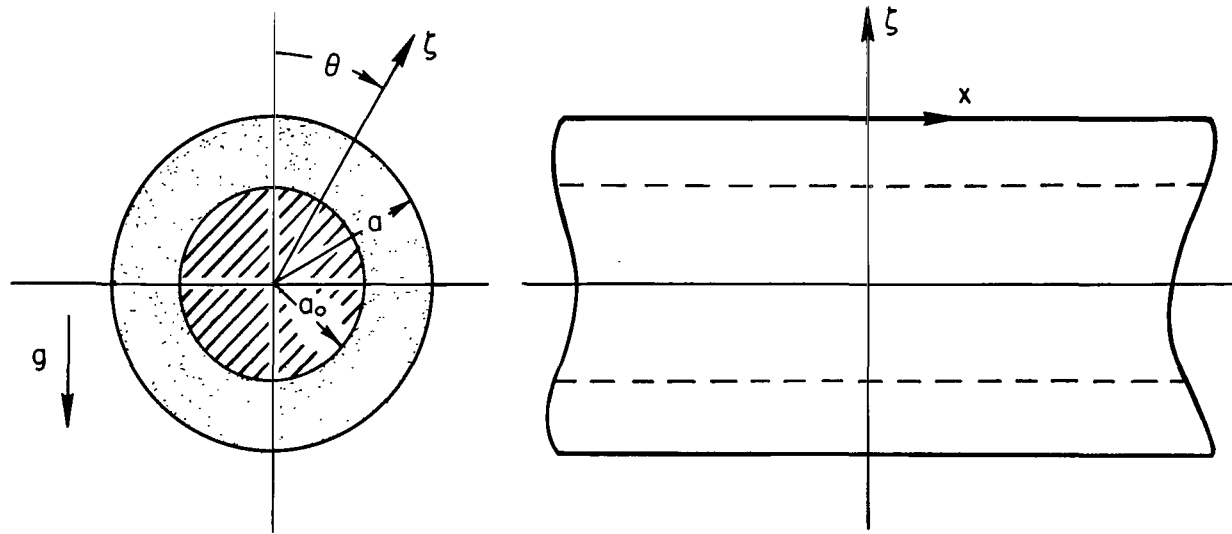


Figure 1.- Sketch of liquid layer and rigid cylinder showing coordinate system.

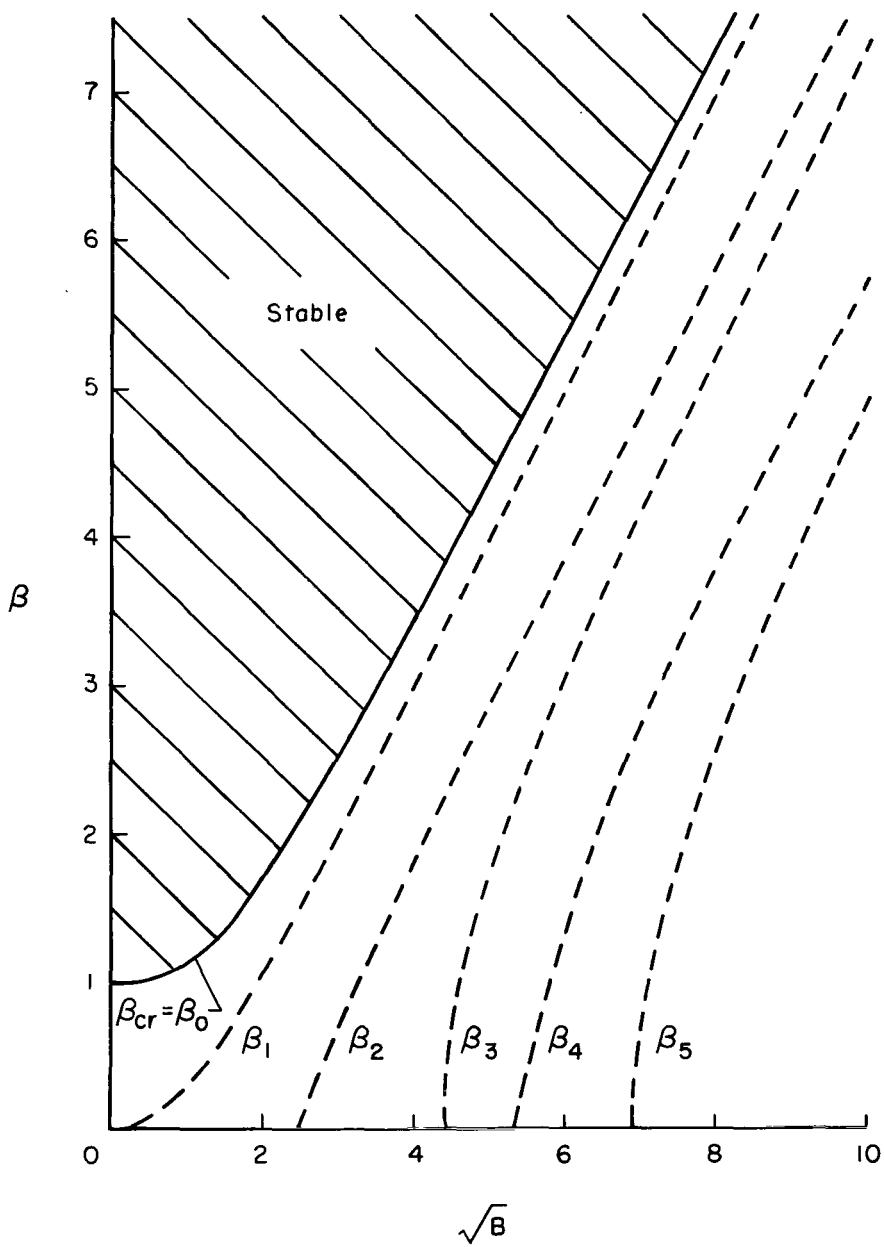


Figure 2.- Stable region of layer as a function of dimensionless cylinder length and Bond number.

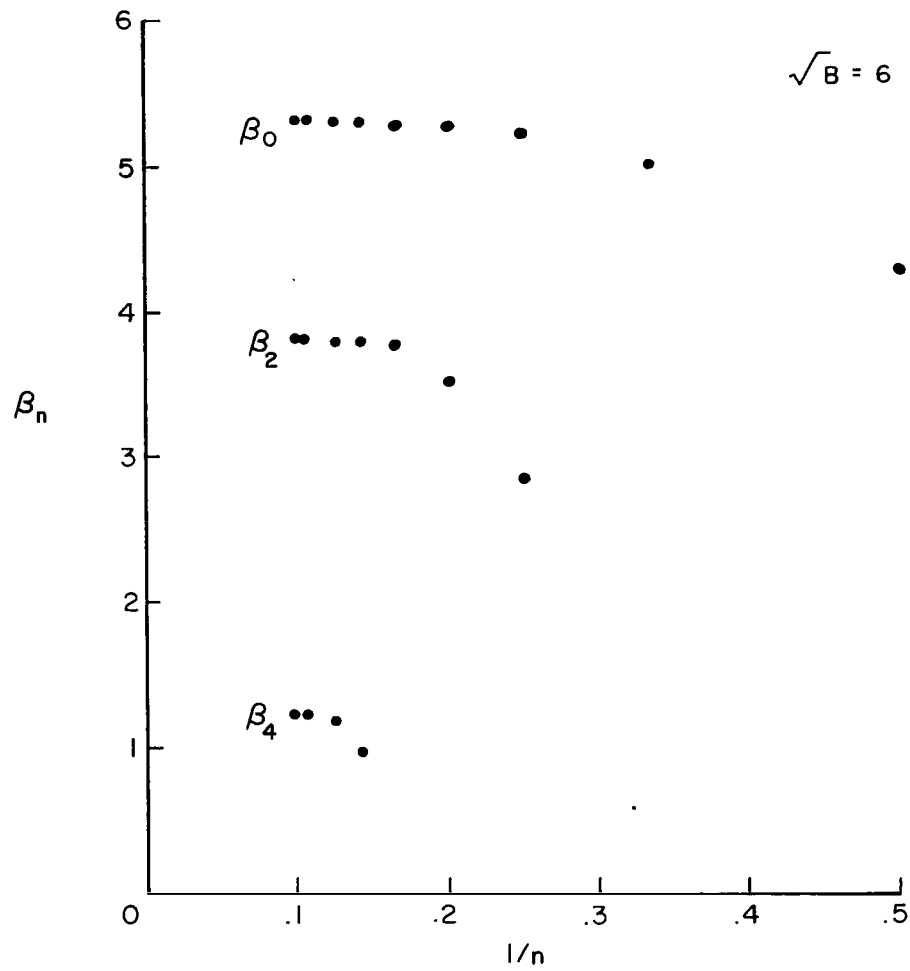
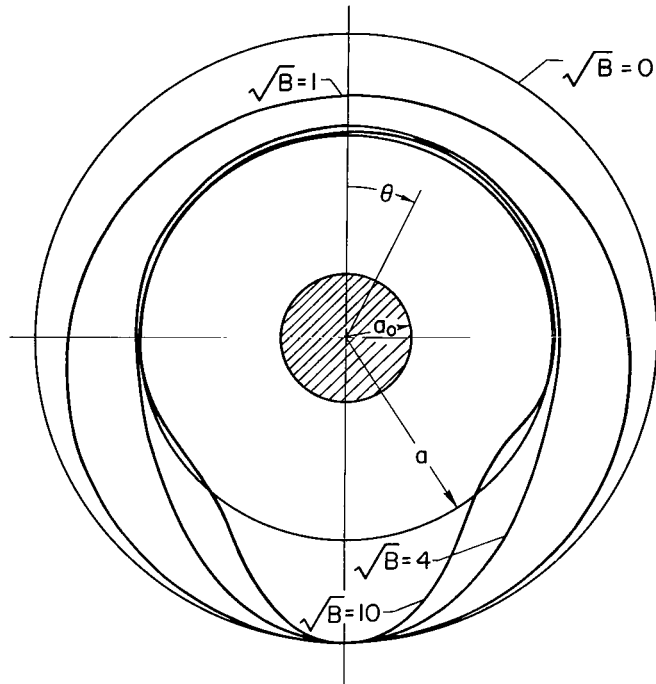
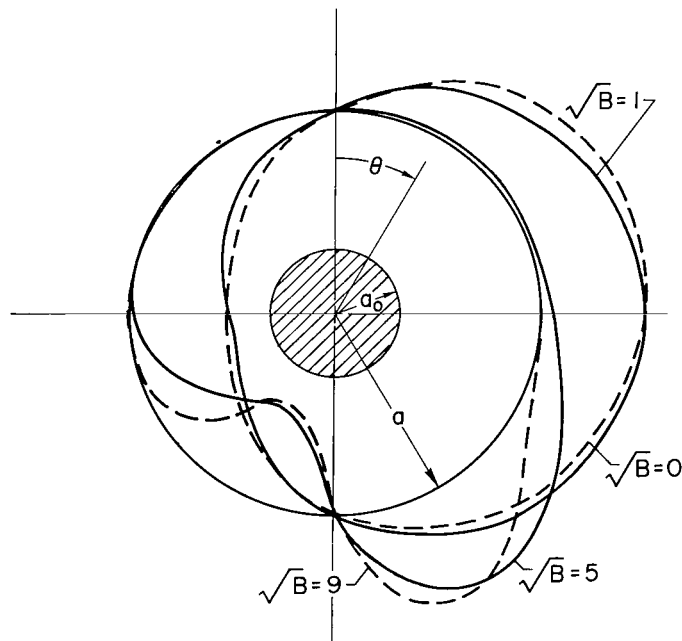


Figure 3.- Plot of dimensionless wavelength as a function of the size of the determinant approximating the infinite determinant in equation (45).



(a) Symmetrical modes.



(b) Antisymmetrical modes.

Figure 4.- Symmetrical and antisymmetrical mode shapes (θ variation) corresponding to β_0 for various values of B . All modes are normalized to the same constant at their maximum values.

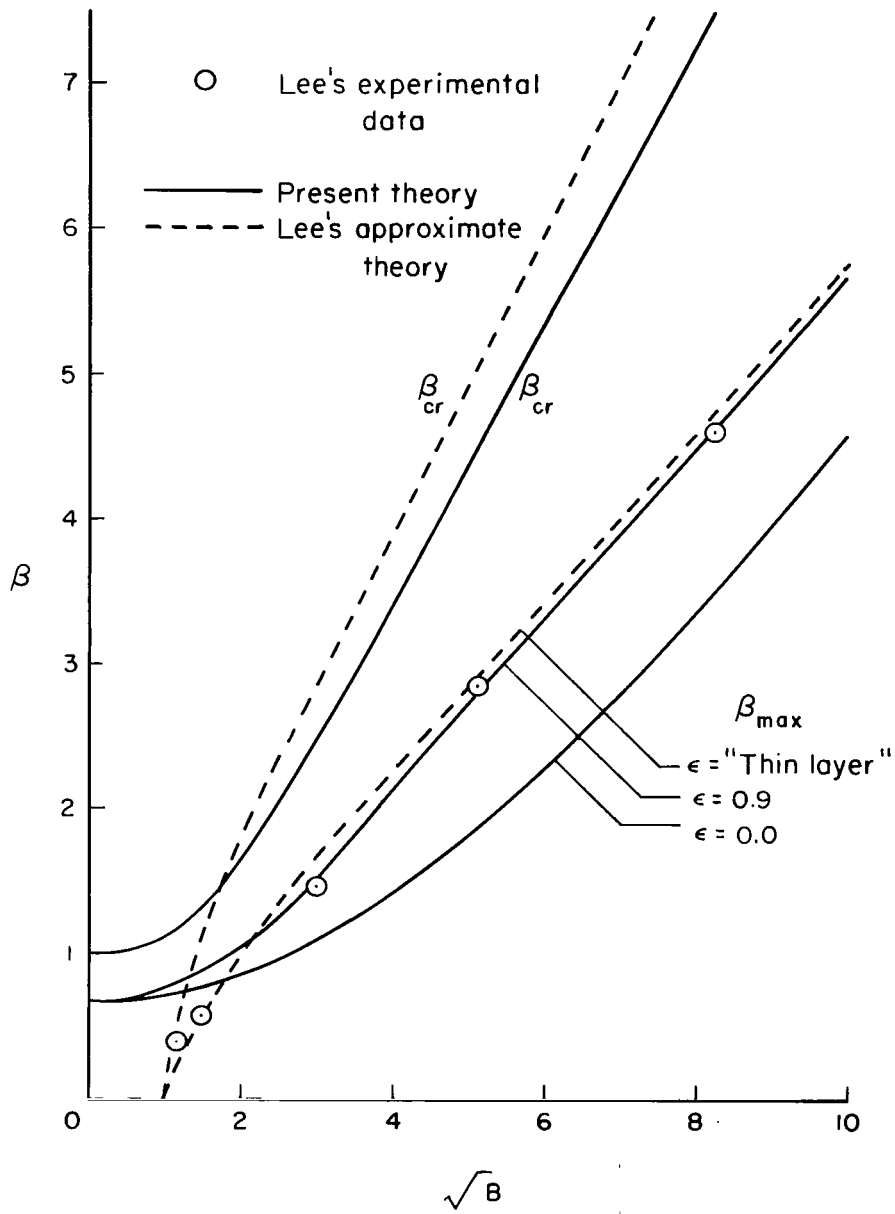


Figure 5.- Comparison of β_{cr} and β_{max} from theories and experiments.

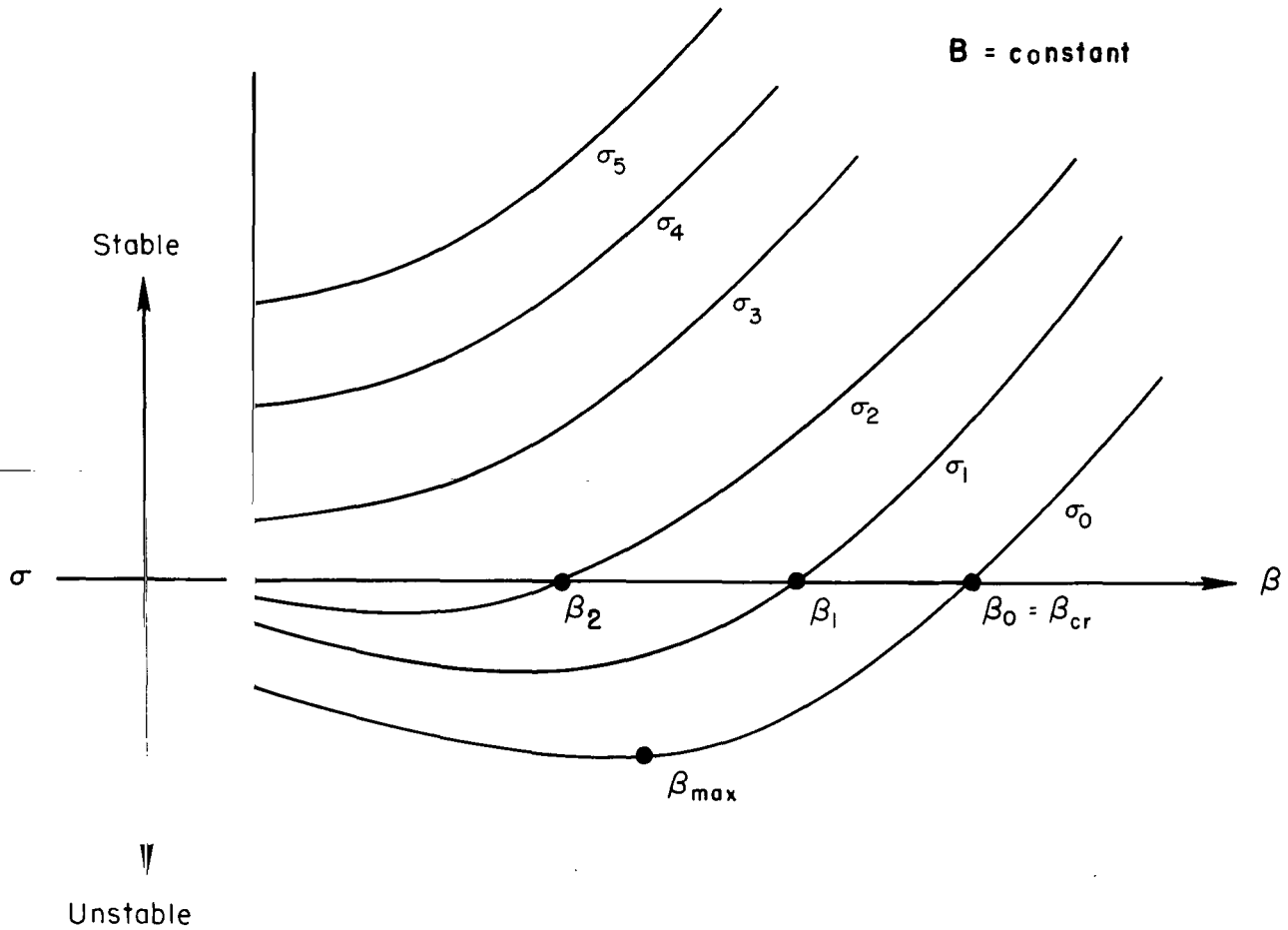


Figure 6.- Typical sketch of $\sigma(\beta)$ for one value of B and indicating β_{cr} and β_{max} .

2/17/25
e

"The aeronautical and space activities of the United States shall be conducted so as to contribute . . . to the expansion of human knowledge of phenomena in the atmosphere and space. The Administration shall provide for the widest practicable and appropriate dissemination of information concerning its activities and the results thereof."

—NATIONAL AERONAUTICS AND SPACE ACT OF 1958

NASA SCIENTIFIC AND TECHNICAL PUBLICATIONS

TECHNICAL REPORTS: Scientific and technical information considered important, complete, and a lasting contribution to existing knowledge.

TECHNICAL NOTES: Information less broad in scope but nevertheless of importance as a contribution to existing knowledge.

TECHNICAL MEMORANDUMS: Information receiving limited distribution because of preliminary data, security classification, or other reasons.

CONTRACTOR REPORTS: Technical information generated in connection with a NASA contract or grant and released under NASA auspices.

TECHNICAL TRANSLATIONS: Information published in a foreign language considered to merit NASA distribution in English.

TECHNICAL REPRINTS: Information derived from NASA activities and initially published in the form of journal articles.

SPECIAL PUBLICATIONS: Information derived from or of value to NASA activities but not necessarily reporting the results of individual NASA-programmed scientific efforts. Publications include conference proceedings, monographs, data compilations, handbooks, sourcebooks, and special bibliographies.

Details on the availability of these publications may be obtained from:

SCIENTIFIC AND TECHNICAL INFORMATION DIVISION
NATIONAL AERONAUTICS AND SPACE ADMINISTRATION

Washington, D.C. 20546